Atmospheric Research 151 (2015) 236–249

Contents lists available at ScienceDirect

Atmospheric Research

journal homepage: www.elsevier.com/locate/atmos

Large fog collectors: New strategies for collection efficiency and structural response to wind pressure

Robert Holmes [a,1], Juan de Dios Rivera [b], Emilio de la Jara [b]

[a] Centro del Desierto de Atacama — Escuela de Diseño, Pontificia Universidad Católica de Chile, El Comendador 1916, Providencia, 7520245, Santiago, Chile
[b] Centro del Desierto de Atacama — Escuela de Ingeniería, Pontificia Universidad Católica de Chile, Av. V. Mackenna 4860, Macul, 7820436, Santiago, Chile

ARTICLE INFO

Article history:
Received 28 October 2013
Received in revised form 6 June 2014
Accepted 15 June 2014
Available online 21 June 2014

Keywords:
Large fog collector
Fog
Water
Fog water
Fog collector screen
Fog collector structure

ABSTRACT

Most studies of large fog collectors (LFC) have focused on the collection efficiency, the amount of water collected, or economic and social aspects, but have not addressed the effects of strong winds on the system. Wind pressure is directly related to fog water collection efficiency but on the other hand may cause serious damage on the structure of LFCs. This study focuses in the effects of wind pressure on the components of the LFC as an integral system, and the ways to face strong winds with no significant damage. For this purpose we analysed cases of mechanical failure of LFCs both in our experimental station at Peña Blanca in Chile and elsewhere.

The effects of wind pressure can be described as a sequence of physical processes, starting with the mesh deformation as a way of adapting to the induced stresses. For a big enough pressure, local stress concentrations generate a progressive rupture of the mesh. In cases where the mesh is sufficiently strong the wind force causes the partial or total collapse of the structure. Usually the weakest part is the mesh, especially close to where it is attached to the structure. The way the mesh is attached to the frame or cable of the structure is particularly important since it can induce significant stress concentrations.

Mesh failure before the structure failure may be considered as a mechanical fuse, since it is cheaper to repair. However, more practical mechanical fuses can be conceived.

In relation to structural performance and water collection efficiency, we propose a new design strategy that considers a three-dimensional spatial display of the collection screen, oblique incidence angle of wind on mesh and small mesh area between the supporting frame. The proposed design strategies consider both the wind pressure on mesh and structure and the collection efficiency as an integral solution for the LFC. These new design strategies are the final output of this research. Applying these strategies a multi-funnel LFC is proposed, which is far more efficient than the conventional one, and even though it is more expensive, the final cost of the collected water should be notoriously reduced.

1. Introduction

The availability of fresh water is one of the most crucial problems for social and economic development around the world (United Nations, 2008) and fog water collection projects could contribute to solve this problem. Fog water collection has been studied and proved for decades as a feasible alternative source of fresh water in semi-arid areas with the presence of suitable persistent fog. This is common in arid and semi-arid areas close to the ocean, where clouds are formed over the sea and then pushed by predominant winds towards the continent, where they turn into fog when

E-mail addresses: rholmes@uc.cl (R. Holmes), jrivera@ing.puc.cl (J.D. Rivera), eadelaja@uc.cl (E. de la Jara).
[1] Tel.: +56 2 23545534.

http://dx.doi.org/10.1016/j.atmosres.2014.06.005
0169-8095/

intercepted by high lands. This kind of fog is addressed as 'advection fog', although sometimes orographic fog also contributes to fog water collection (Cereceda et al., 2002, 2008b). Several studies have recognised the potential of fog water collection for human consumption around the world, in places such as: Pacific coast of northern South America (Cereceda et al., 2008a,b, 2002; Larrain et al., 2002), the Canary Islands (Marzol, 2002, 2008), Morocco (Marzol and Sánchez, 2008), South Africa (Olivier, 2002; Olivier and de Rautenbach, 2002; Louw et al., 1998), Oman (Abdul-Wahab and Lea, 2008; Abdul-Wahab et al., 2010), Saudi Arabia (Al-hassan, 2009; Gandhidasan and Abualhamayel, 2006), western Mediterranean basin (Estrela et al., 2008), and Namibia (Shanyengana et al., 2002).

Since the first studies made by Carlos Espinosa in Chile, 1957 (Gischler, 1991), fog water collection projects had relied on different designs of fog collection devices, where the flat screen large fog collector (LFC, see Fig. 1) is the most common type of design used in the last decades (Schemenauer et al., 1988; Schemenauer and Cereceda, 1994b; Gischler, 1991). The materials used for the LFC are usually simple components, locally available, because the main focus of fog water collection projects has been to provide fresh water to small, poor communities around the world. These projects have been mainly supported by non-governmental organizations (NGO), which are responsible to install the system (Klemm et al., 2012; Schemenauer et al., 2005).

One of the main problems that affects the sustainability of fog water collection projects is maintenance of the LFC that are frequently damaged by strong winds events, the sun (UV radiation) and other environmental factors which affect the structure, mesh and other components (Schemenauer et al., 2005). Since the collection systems are usually installed in poor communities in developing countries, personnel in charge of maintenance have neither the technical nor the economic resources to repair them and, eventually, this implies the abandonment of the project (de la Lastra, 2002).

Recently, Klemm et al. (2012) made a thorough review of existing LFC installations around the world. However, they did not analyse in detail the effects of wind pressure on the

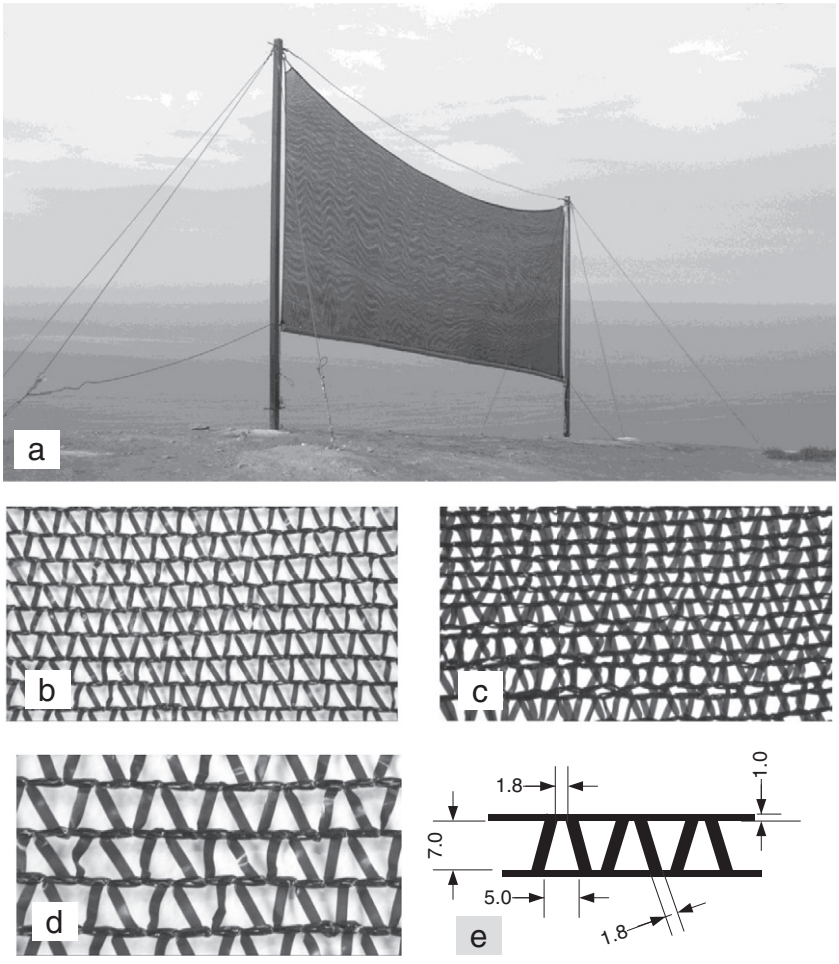

Fig. 1. a: The most common type of design for a large fog collector (LFC), based on a flat screen, has been used for decades. Example of a flat screen LFC at Alto Patache, Chile. b: Single layer Raschel mesh, 35% shade coefficient. c: Double layer Raschel mesh, 35% shade coefficient each layer, notice the uneven local shade coefficient resulting from the overlapped meshes. d and e: Details and dimensions in millimetres of the structure and the filaments of a typical Raschel mesh (www.marienberg.cl).

mesh and the supporting structure, and the effect of design variables on water collection efficiency. Indeed, it is noteworthy that, as far as we know, no peer review publication has dealt with the currently observed mesh breakage or structural collapse of LFCs caused by extreme winds.

The issue of collection efficiency of LFCs has been scarcely treated until recently. The first study on efficiency was by Schemenauer and Joe (1989) and some study of the airflow around and through the collector was made by Bresci (2002). Recently, Rivera (2011) deduced a theoretical model for the aerodynamic collection efficiency as a function of the mesh shade coefficient, and de la Jara (2012) arrived to similar results by numerical modelling of a two-dimensional mesh. Finally, Park et al. (2013) demonstrated the relevance of the mesh material wetting angle and its hysteresis in the mesh design and efficiency. The efficiency of small fog collectors used to obtain samples of fog water to study its characteristics has been analysed by several authors (i.e. Michna et al., 2013), but they are not directly applicable to our case because they are active collectors that draw air by mechanical means.

In this area of the fog water collection experience, the interdisciplinary team of the Centro del Desierto de Atacama of Pontificia Universidad Catolica de Chile integrated by geographers, engineers, architects and industrial designers, has developed a research programme in three complementary lines: practical work in the experimental stations of Alto Patache, Peña Blanca and Majada Blanca in northern Chile, experimental work and testing in the laboratories of the School of Engineering at Pontificia Universidad Catolica de Chile and at Universidad de los Andes, and computational modelling and analysis of aero-hydrodynamics and structural behaviour of the mesh and the supporting structure. This programme has produced preliminary results that pose new questions for future research.

In this paper we review models for estimating wind force on the LFC, analyse some actual cases of LFC where notorious mesh damage and structure collapse occurred, and propose new design strategies. The proposed strategies aim to optimise the structural response to wind pressure and to minimise maintenance, which is one of the main problems for the sustainability of fog collection projects. These strategies are also focused in optimising collection efficiency by modifying the mesh spatial display and the consequent aerodynamic behaviour.

Section 2 comments on the background of previous experiences related to LFC exposure to wind forces, especially as gale force winds, and the liquid water flux as a background for this research. Section 3 discusses the wind effects on LFCs in relation to collection efficiency, wind force and the eventual failure of the LFC. Discussion of collection efficiency starts briefly describing the concept. Next, we review models for estimating wind pressures on the mesh and finally, we analyse its effects on the failure of the mesh itself and the supporting structure. Section 4 presents results of tensile tests for Raschel mesh related to the observed behaviour of a number of LFCs, enumerating the typical problems and failures. Section 5 presents and discusses the new design strategies proposed to solve the problems induced by strong winds, and estimates the collection efficiencies that these kind of design could have. The proposed fog water collector has been analysed by numerical simulations of wind force and collection efficiency, which presents very promising results. The new LFC has not been built as yet. Finally, in Section 6, several conclusions are driven, in order to apply the new concepts for LFC design.

2. Background

The structure of LFCs must withstand different types of forces. First, there are gravitational forces, corresponding to the dead weight of the wet mesh, cables, trough full of water and other structural elements. Also, there are dynamic loads corresponding to erection and maintenance of the system. Additionally, there may be seismic loads in places like Chile. However, the largest and most significant load is wind. Most frequently, LFCs are installed in windy places because only wind driven fog permits water collection (Schemenauer and Cereceda, 1994a; Schemenauer and Joe, 1989). Indeed, what really matters is the liquid water flux, which can be expressed as the liquid water content (LWC) times the wind speed. Therefore, stronger winds imply larger liquid water fluxes for the same LWC, which results in a higher potential for water collection. Additionally, the impact, or deposition, efficiency increases with wind speed (Schemenauer and Joe, 1989; Park et al., 2013). On the other hand, one of the problems faced by LFCs is destruction produced by gale force winds (over 17 m/s, no 8 in Beaufort wind scale) or stronger. The frequency of these gale force winds depends on the particular site. However, since the sites are usually in the top of a mountain or in saddle points, strong winds are more frequent than in lower places where meteorological stations are usually located. For this reason, there is no valid statistical information available for the actual location of LFCs. However, as a reference, we can mention that in the El Tofo–Chungungo project, wind storms destroyed some LFCs every 2 to 5 years (de la Lastra, 2002), and in Peña Blanca wind storms come every 2 years. In summary, wind is an ally and a foe at the same time.

Large fog collectors represent an obstruction to wind flow and, therefore, part of the wind flows around the mesh, as shown in Fig. 2. The fraction of the flow that goes around the LFC depends on the resistance of the mesh to airflow, that is characterised by its pressure drop coefficient, C_0, and on the

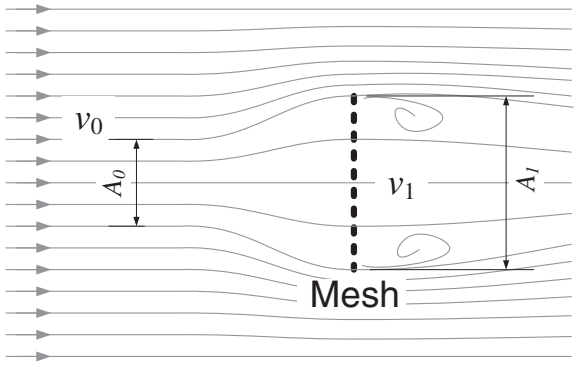

Fig 2. Airstreams through and around the mesh of an LFC. The total area of the mesh, A_1, is larger than the area of the stream tube that effectively passes through the mesh, A_0. The air velocity v_0 is the unperturbed wind velocity, and v_1 is the velocity of the wind actually going through the mesh.

mesh aspect ratio and other three-dimensional characteristics of the LFC (Rivera, 2011). The pressure drop coefficient depends on the mesh shade coefficient and the aerodynamic characteristics of the filaments and weaving or knitting pattern. All these factors affect both wind forces on the mesh and the collection efficiency.

The specification of the unperturbed wind velocity, v_0, is not straightforward because of the atmospheric boundary layer velocity gradient (Petersen et al., 1998). Indeed, velocity increases with height, although most models for calculating LFC efficiency, rate of collection and wind force consider a uniform velocity. A common practise is to use the velocity at the centre of the mesh. Also, the effect of the ground, both in terms of the flow pattern and turbulence, is sometimes acknowledged but frequently ignored. Heisler and Dewalle (1988) make a thorough review of the effects of windbreak structures on wind flow that can be applied to a large extent to LFCs.

In the following sections we analyse the factors affecting collection efficiency, then, we review methods to estimate the wind force on LFC and, finally, we analyse the effects of this force on the mesh and the structure.

3. Materials and methods

The efficiency of an LFC, as defined by Schemenauer and Joe (1989), is the ratio of the collected water to the available liquid water flux in the undisturbed fog. This efficiency can be factored into three other efficiencies (Rivera, 2011), the aerodynamic collection efficiency (ACE), the capture efficiency, and the draining efficiency. The capture efficiency is also called, perhaps more appropriately, deposition efficiency by Park et al. (2013). The aerodynamic collection efficiency (η_{AC}) is the fraction of the unperturbed liquid water flux heading towards the LFC that would collide with the mesh filaments, which is a function of the mesh shade coefficient (s), its pressure drop coefficient (C_0), and the drag coefficient of the LFC if fitted with a non-permeable screen, (C_d), as shown by Eq. (1).

$$\eta_{AC} = \frac{s}{1+\sqrt{C_0/C_d}} \tag{1}$$

Deposition efficiency accounts for the interaction of droplets with the mesh fibres, since droplets tend to follow the air streamlines; it is a function of Stoke number. Deposition efficiency increases with decreasing fibre diameter and increasing wind speed. Draining efficiency takes into account that not all the water deposited on the fibres will reach the gutter at the bottom of the mesh because some will be lost by re-entrainment and spills. The complex effect of mesh material wetting angle, mesh design, droplets diameter and wind speed on collection efficiency is analysed by Park et al. (2013).

3.1. Wind pressure on semi-permeable screens

In order to perform the structural analysis of the LFC, it is necessary to know or estimate the pressure exerted by the wind on the mesh. Wind forces on porous surfaces have been studied in relation to wind break fences, bird canopies for horticultural crops, shade houses and hail shelters. Richards and Robinson (1999) reviewed the experimental and theoretical work done at that time on wind forces on semi-permeable screens. They express this force (F), as customarily, using a drag coefficient C_D:

$$F = C_D \rho \frac{v_0^2}{2} A_1, \tag{2}$$

where ρ is the air density, v_0 is the unperturbed wind speed and A_1 is the screen area projected onto a plane normal to the wind velocity. The drag coefficient is a function of the LFC aspect ratio, i.e. the ratio between its height and length, and mesh flow coefficient k, equivalent to the pressure drop coefficient C_0 used by Rivera (2011), which gives the pressure drop Δp of a flow across the mesh:

$$\Delta p = k \rho \frac{v_1^2}{2}, \tag{3}$$

where v_1 is the speed of the wind passing across the mesh. This flow coefficient depends on the shade coefficient (s) and the characteristics of the mesh pattern and the filaments. In their paper they use porosity ($\beta = 1 - s$), instead of shade coefficient, but we opted for the latter because it is the usual way to characterise the mesh for LFC. For a square mesh pattern with round wires of diameter d, and filament Reynolds number ($\mathrm{Re} = \rho v_1 d/\mu$) greater than 2000, they give the following equation for k:

$$k = \left[\left(\frac{s}{1-s} \right)^8 + \frac{s^4}{(1-0.75s)^8} \right]^{0.25} \tag{4}$$

Since in most LFC, with filament diameters of the order of 1 mm and velocities of the order of 5 m/s, Re is of the order of 300, they give a correction for lower Re.

$$k(\mathrm{Re}) = k(\mathrm{Re}{>}2000)\left(1 + 14.5/\mathrm{Re}^{0.75}\right) \tag{5}$$

Since typical meshes used for LFC have neither round wire nor square pattern, they recommend measuring the loss coefficient in a wind tunnel and calculating an equivalent shade coefficient (s_e) to be used in the previous equations. Nevertheless, they recommend for 5 mm wide flat filaments, which closely corresponds to the ones in Raschel mesh, to use an equivalent shade coefficient $s_e = (1 + 2\,s)/3$. Finally, based on full-scale and wind tunnel measurements they suggest a simple relation for the screen drag coefficient C_D as the product of the effective shade coefficient and the drag coefficient C_{D-np} of a non-permeable screen:

$$C_D = s_e C_{D-np} \tag{6}$$

Therefore, the procedure to calculate the wind force on an LFC would be to measure the flow coefficient, k, of the particular mesh used at a wind speed similar to the one expected, then with Eq. (4) obtain the effective shade coefficient, next calculate the drag coefficient with Eq. (6), and, finally, calculate the force with Eq. (2). If it is not possible to measure the flow coefficient, use directly Eqs. (6) and (2).

3.2. Effect of oblique wind

Richard and Robinson also analyse the case when the wind is not perpendicular to the mesh, defining the incidence angle (θ) as the angle between wind direction and the normal to the screen. After comparing several semi-empirical correlations with empirical data, they conclude that, for shade coefficients in the range 0.5 to 0.7, typical of LFCs, the most convenient correlation is

$$C_D = C_D(\theta = 0)\cos\theta \tag{7}$$

Some later publications that deal with the drag and lift coefficients of porous roofs (Letchford et al., 2000; Uematsu et al., 2008) or signboards (Letchford, 2001) could be relevant to LFCs, but the conditions are quite different and, therefore, are not directly applicable. Indeed, they consider shade coefficients over 0.77 and incidence angles quite high, over 73°. Additionally, as they recognise, roof structural details can have a significant effect on the drag coefficient. Nevertheless, Uematsu et al. (2008) make a gust wind effects analysis and Letchford (2001) studies the effect of screen clearance distance from the ground on the drag coefficient, both results are quite applicable to LFCs.

Giannouilis et al. (2012) made an updated review of the state of the art in wind force calculation on porous panels, concluding that Eqs. (4) and (5) are still the best, considering a significant disagreement between different experimental results. This is attributed to the fact that most studies use porosity, or shade coefficient, to characterise the porous screen, but porosity by itself is not enough to describe its aerodynamic behaviour. The pressure drop coefficient across the mesh is a better characterisation. However, this coefficient is laborious to obtain and normally it is not known for the vast majority of the materials used in practise and in the experimental work for which data is available. They also make the difference between reported pressure coefficient and force, or drag, coefficient, since the former relates to the ratio of the upwind and downwind local pressure close to the screen or mesh, which is not uniform over its surface. They summarise the results of Letchford (2001) that experimentally showed that the drag coefficient increases in elevated panels that have a clearance between the lower edge and the ground. They conclude that the mean drag coefficient for non-permeable screens with aspect ratios larger than 0.5 lies between 1.05 and 1.20, but they increase from 1.4 to 1.5 in elevated panels with clearing ratio (distance between the bottom of the screen and the ground divided by the height of the screen) over 0.6. No conclusions were drawn concerning the effects of clearing ratio, wind incidence angle and porosity for elevated panels because of disagreement of the scarce results so far published.

In summary, for our calculations of the wind load over the fog collector, assuming a clearance ratio smaller than 0.6, we will consider the force coefficient for non-porous panel equal to 1.05 and an air density of 1.15 kg/m^3 (94 kPa, 11 °C, 600 m.a.s.l.), which gives

$$F = 1.05 \cdot s \cdot 1.15\frac{v_0^2}{2}A_1 = 0.604 s v_0^2 A_1 \tag{8}$$

4. Results

Wind behaviour is dynamic, so design strategies must consider the extreme situations of these events to generate an adequate responsiveness to these demands in LFCs. Strong wind gusts may be present in very short periods of time (Briassoulis et al., 2010; Agustsson and Olafsson, 2009; Boettcher et al., 2003; Walshaw and Anderson, 2000; Weggel, 1999) but may cause important damage.

To have a more accurate data of liquid water content (LWC) times the wind speed, a Ground-Based Environmental Sensing and Fog Collector Monitoring System (ESAMS) was designed, tested and deployed in the experimental station of Majada Blanca (LeBoeuf et al., 2013). Wind speed observations can be averaged in different periods of time. For example, in Fig. 3 we can observe a period of 24 hours that shows this dynamic behaviour of the wind expressed by a sequence of wind gusts.

In the different types of weaving or knitting, the directionality of the fibre is relevant to the structural behaviour of the mesh. This is especially notorious in the asymmetrical knitting configuration of the Raschel mesh, which is the one we considered in this specific research. This implies an anisotropic behaviour of the mesh that presents a much higher modulus of elasticity and ultimate tensile strength along than across the knitting direction, as shown in Fig. 4. Indeed, in this direction the stiffness per unit width is 17,500 N/m with a stretching at the rupture point of 20% of the initial length, and across the stiffness is 900 N/m with a rupture stretching of 100%. The stiffness is the slope of the curves shown in Fig. 4.

In the analysis of various cases, we have observed that the strong wind pressure on the LFC generates two important problems in the collection screen (Raschel mesh):

(a) mesh deformation, both elastic and plastic, produces sagging
(b) stress concentration in critical areas generates local breakage and consequent openings in the mesh that will grow until total destruction.

The different possibilities of mesh failure work as unintended fuses to liberate the wind pressure. In some occasions, when the

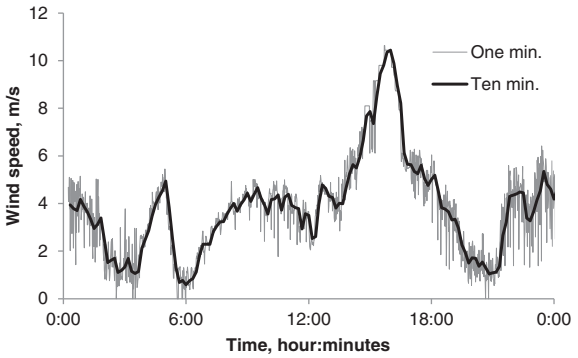

Fig. 3. Twenty-four-hour wind speed observation at Majada Blanca, Chile (30°03′56″ S, 71°19′19″ W, 699 m.a.s.l., time zone: UTC-4), December 17th, 2012. The black trace represents ten-minute averages, and the light grey trace represents one-minute averages.

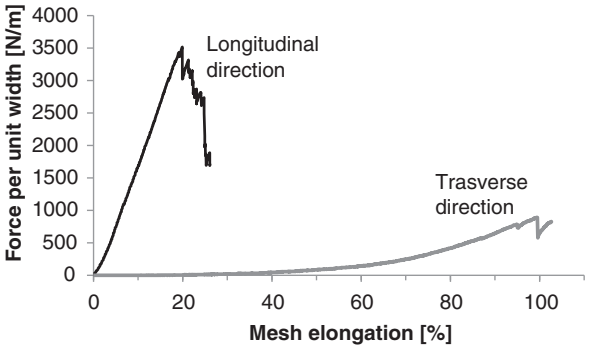

Fig. 4. Tensile test of Raschel mesh, 35% shade coefficient. Longitudinal direction corresponds to the knitting direction.

mesh can resist the stress, the extreme force is transferred to the supporting structure and, eventually, to the base of the structure.

4.1. Sagging

Sagging is a deformation of the flat mesh into a parabolic surface as a consequence of the elastic and plastic deformation generated by wind pressure, as shown in Fig. 5. For this induced parabolic shape, the drag coefficient increases and so does wind pressure and, as a consequence, stress on the mesh material also increases. On the other hand, according to Eq. (1), collection efficiency should also increase because of the increasing drag coefficient. However, in some occasions we have observed water dripping in the lower part of the sagged mesh, which is lost because it falls out of the trough. Unfortunately, no measurement of this loss has ever being made and, therefore, we do not know how important it is. In conclusion, sagging is bad from the structural point of view but may be good, to a certain extent if there is no spilling, for collection efficiency.

Sagging increases in proportion to the distance to the peripheral attachment of the mesh and decreases with stiffness of the mesh and the structure. This means that for larger surfaces and smaller stiffness sagging is more prominent. Sagging of a mesh surface can be quantified by the curvature $C = 1/R$, where R is the radius of the smallest circle that can be approximately fitted to the curved mesh. We are not currently aware of any publication reporting measurements of the amount of sagging produced in different LFCs, or its effect on the structure collapse or the collection efficiency. For this reason, we plan to measure both effects in a new LFC we recently installed, that is being fully instrumented. Sagging could finally generate a permanent deformation and the consequent flaccidity of the mesh. This flaccidity generates an alteration of the desired shade coefficient and may reduce the draining efficiency.

4.2. Rupture by stress concentration on mesh attachment areas

In most cases the screen is attached to a rigid frame or to a tense cable frame. The fixation can be defined as a sequence of discrete points or as continuous attachment. In the first case, we have to consider stress concentration in those points, whilst in the continuous attachment, ideally, stresses are distributed homogeneously. These stresses are directly proportional to the distance between the attachment points and to a stress concentration factor that depends on the details of the particular attachment system and the mesh. The initial rupture of the mesh is produced close to the attachment points and will progressively expand through their neighbourhood, as shown in Fig. 6a, and its expansion is enhanced by the cyclic nature of wind induced forces.

Fig. 5. Wind pressure generates sagging, an elastic and, eventually, plastic deformation of the collection screen (mesh) of the LFC. Example of LFC in Majada Blanca, Chile.

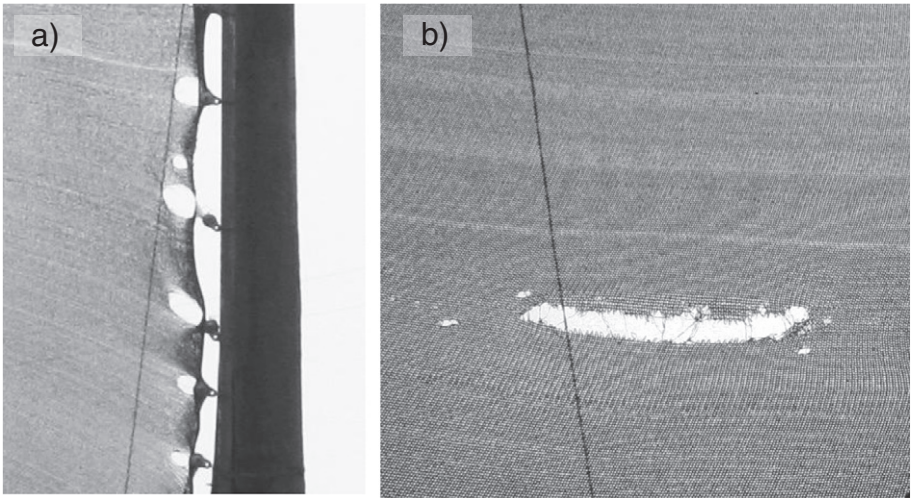

Fig. 6. Wind pressure may generate stress concentration in attachment areas (a), initiating a mesh rupture. Rupture can also be initiated far from the attachments (b), the characteristics of this rupture will depend on the anisotropic behaviour of the mesh (Raschel mesh). Example of LFC in Peña Blanca, Chile.

4.3. Rupture by stress on material heterogeneity of mesh in unpredicted areas

The characteristics of this rupture will depend on the anisotropic or isotropic configuration of the mesh knitting and/or because of material weakness. Fig. 6b shows the case of Raschel mesh that has an anisotropic configuration. If we consider the anisotropic configuration of the mesh it is possible to predict that rupture will occur parallel to the direction of the strongest fibres, as the weakest fibres in the other direction will fail first. In an isotropic configuration, the mesh rupture will occur as a consequence of material weakness, and as to where it will start, it is unpredictable.

4.4. Extended mesh surface rupture

The extended mesh rupture, especially when the drag coefficient increases by sagging, can be seen as a progressive process of disintegration by rupture of the mesh fibres and of the knitting structure. This extended rupture has its origin in the particular stress concentration areas or in the unpredicted areas due to anisotropic behaviour, abrasion due to rubbing against another object or material weak spots in some area of the mesh. In these cases the complete rupture of the mesh will work as an extreme fuse, liberating pressure on the supporting structure, as shown in Fig. 7. This will permit the user to re-install new meshes, saving the supporting structure.

4.5. Structure collapse

When the collection screen is tough enough to resist the wind pressure, the force is transmitted to the supporting structure, which may fail in the weakest components or joints, as shown in Fig. 8a. If the supporting structure can resist the derived stress from the collection screen, all stresses are finally concentrated at the weakest point of the structure, often the base of cantilever poles if the stay cables have already failed, so the whole installation may collapse as a monolithic body, as shown in Fig. 8b that presents the case of Anagua Project, Canary Island.

5. Discussion

Considering the general wind flow conditions, velocity, turbulence, intermittency, to which LFCs are normally exposed, and the consequent effects on the collection screen and supporting structure, we propose a new design strategy that will respond efficiently to these conditions. This strategy is based in three concepts: (a) three-dimensional configuration of mesh and structure, (b) oblique incidence angle of wind on mesh, and (c) small mesh area between the supporting frames. Applying this strategy we propose a particular design, which was analysed with numerical simulation. In parallel to this new strategy, we are working on improvements to the more conventional design, like the one illustrated by Fig. 1, installed at the experimental site of Majada Blanca (30°03′56″ S, 71°19′19″ W, 699 m.a.s.l.) shown by Fig. 5. The new features of these LFC are enlarged size (150 m^2 of mesh area), pivoting poles and highly flexible structure. The results will be published in due time.

In this section we first analyse this new design for the LFC that consists of a modular funnel device with an open vertex with a sleeve. This new design will now be referred to as modular funnel-large fog collector (MF-LFC). Then we analyse the numerical simulations of pressure release and collection efficiency concerning this MF-LFC design. This analysis presents relevant information to prove the benefits of this new design.

5.1. Three-dimensional funnel device with an open vertex with a sleeve

The new proposed design is based on a three-dimensional funnel device configuration generated by two converging

Fig. 7. Wind pressure may generate an extended mesh rupture when the force exceeds the tensile resistance of the fibres. It may start in localised areas, but it will develop as a progressive process of disintegration. Example of an LFC in Peña Blanca, Chile.

screen units confronting the predominant wind direction at an oblique angle. This funnel morphology guides the wind driven fog flux to an enclosed space with a sleeved opening at its vertex that conducts the wind flow out of the system. The design of this opening is based on deployable multi-tubular sleeve membrane, as shown in Fig. 9.

The most relevant functional properties of this new design for the MF-LFC are the following:

5.1.1. Increase of collection area

This design strategy provides a much larger area for the collection screen in relation to the traditional frontal collection plane exposed to the wind direction. This new geometry improves the relation between the collection surface area and fog flux cross sectional area.

5.1.2. Oblique impact of water drop on collection screen

This oblique position of the mesh in relation to the wind driven fog flux direction also increases collection efficiency due to the modification of the impact angle, as was found by de la Jara (2012) and further demonstrated in Section 5.2 (Collection efficiency).

5.1.3. Modification of fog flux through the collector

This design offers an improvement of the fog flux in relation to the traditional, flat, LFC version where the average wind speed at the mesh surface is lower due to the blockage effect. The new design improves water collection due to the increase of the drag coefficient and by providing flux continuity, modifying the aerodynamics of the traditional LFC.

To estimate the efficiency of this design, numerical simulations were performed to compare the traditional flat frontal plane screen to the proposed funnel morphology with open and closed vertex. Some details on the simulations are discussed below.

a) Destruction of structural components when forces are transmitted from the collection screen to the supporting system. Example of LFC in Peña Blanca, Chile.

b) Structure collapses at the base (Anagua project - Canary Island, with permit by Carlos Sanchez Recio).

Fig. 8. When the collection mesh resists wind pressure, the structure may fail.

5.1.4. Mesh resistance to wind pressure

The structural response of the mesh to the wind pressure is more efficient, as each of these oblique mesh units that configure the funnel device are rather small surfaces compared to the large surfaces of the traditional LFC. Therefore, considering the small extension of the mesh between the peripheral fixations, fibre stress will diminish and so do the consequent sagging and eventual rupture of the mesh.

5.1.5. Tensile structure and modular addition

The design strategy for the tensile structure (also called *tensegrity*) improves the efficiency of the MF-LFC in relation to the minimum material required and the resistance to the stresses due to strong winds, as shown in Fig. 10. This improvement has a direct impact on the material resources, production, erection and maintenance processes, which finally affects the total cost of collected water.

The MF-LFC is configured by the addition of these modular funnel devices that generate a large multi-modular screen with several units between supporting posts, permitting the control of the catenary curve deformation due to own weight, the added weight of collected water on the mesh and the wind pressure on the screen surface. From the point of view of collection efficiency, this novel design should be superior to the flat LFC over a typical range of wind speeds (4 to 10 m/s), since even for a 2 m/s wind the flow is fully turbulent (Reynolds number ~ 700,000).

The materials used for the supporting tensile structure are tubular poles of zinc plated carbon steel, for the vertical and horizontal compression elements, zinc plated steel cables and fittings for the traction elements. For the collection surface we consider alternatively a 2 mm wide ribbon, double layer Raschel mesh (35% shade coefficient) or a 1 mm mono-filament single layer Raschel mesh (50% shade coefficient).

As the design concept is based on the addition of modular funnel units, the frontal length of the fog collector can be variable but for the optimisation of the tensile structure we recommend a span of 14 m between vertical posts which can be installed in a variable sequence of frontal alignment. The total height of the collector is variable, although normally between 6 and 9 m.

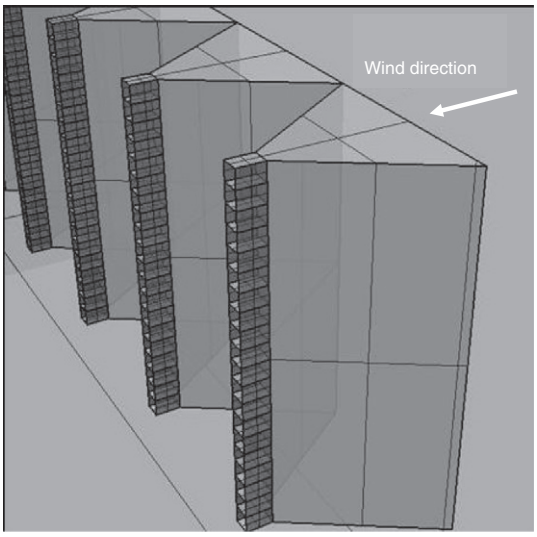

Fig. 9. Three-dimensional funnel device with an open vertex with a sleeve. Wind blows into the funnel pushing fog droplets against oblique screens.

5.2. Numerical simulations: Pressure release and collection efficiency

A set of numerical simulations were performed to estimate the effects of the pressure fusses on the drag force and aerodynamic efficiency for the proposed MF-LFC shown on Figs. 9 and 10. The focus of the simulations is to evaluate the potential effects of new design strategies. The following sections describe the numerical simulations made by computational fluid dynamics (CFD) models, using the CFD module of the Software Comsol Multiphysics, Version 3.5a (Comsol, 2008) and analyse its results. In order to validate the simulations, the drag force simulated on a flat LFC was compared to empirical correlations. The main goal of these numerical simulations is to estimate and analyse the performance of new design strategies proposed in this work. Three different LFC geometries were analysed: flat screen, closed funnel, and open funnel.

5.2.1. CFD modelling setup

The CFD models developed for this work are based on a two-dimensional simplified geometry of a large fog collector. The Reynolds Average Navier Stokes (RANS) equations, coupled with a k-ε turbulence model, were solved for each LFC geometry to estimate the trajectories of fog droplets and the wind pressure over the structure. These numerical simulations are similar to the ones performed by de la Jara (2012). The main objective of the CFD models is to estimate, in orders of magnitude, some variables of interest, such as aerodynamic collection efficiency and pressure over the LFC structure.

The main constants for the model setup are summarised on Table 1, and the following section describes the results of the three CFD simulations.

5.2.2. Wind pressure

Three different CFD simulations were performed assuming that the structure is not deformed by the wind. These simulations are a first approach for the pressure estimation, because as the wind blows over the structure, it produces an elastic, or plastic, deformation on it that changes the shape effects on the drag coefficient. The results of the velocity fields of the three different geometries are shown in Fig. 11.

The total pressure over the structure can be estimated by integrating the velocity and pressure fields. The results of the total pressure over the un-deformed structures are shown in Fig. 12.

The empirical correlation for wind forces given by Eq. (8) is used to validate the simulations for the flat mesh. The difference between the correlations and the CFD simulations for the flat mesh is 16.6%, giving an acceptable agreement. Eq. (8) is applicable to any structure with a known drag coefficient for non-permeable screens. Therefore, since we do not know the drag coefficient for the structures corresponding to the MF-LFC geometry proposed in this work, we cannot use this correlation. However, White (1986) gives a drag

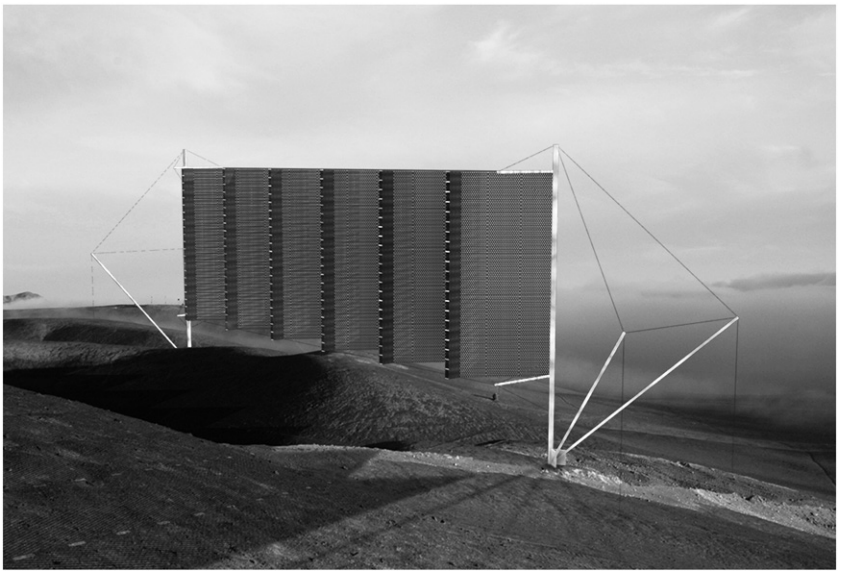

Fig. 10. Multi-modular funnel LFC, displayed and supported by a tensile structure. Render of a proposed MF-LFC.

coefficient of 2.3 for a C-shaped structure, which can be considered similar to the closed MF-LFC. If we use Eq. (8) with this drag coefficient we obtain a force of 39.7 N/m, which is of the order of the simulation results (10% difference). With the velocity fields, it is possible to track the trajectories of fog droplets interacting with the LFC structure, as described in the following section.

5.2.3. Collection efficiency

The collection efficiency can be estimated by tracing the trajectory of fog droplets in the control volume and identifying the fate of each one. Since we did not simulate water draining down the mesh, our simulation assumes 100% draining efficiency. The trajectories of a large number of discrete droplets, entering the control volume at the same speed of the wind, are determined by solving the equations for the interaction between the inertial and viscous forces (drag) affecting each droplet, over time, and through the control volume, resulting in different trajectories for each droplet with its end point identified. The collection efficiency can be estimated dividing the number of droplets that impact the fibres by the number that entered the control volume through an area of the same magnitude as the collector projected area. Therefore, the efficiency for every case considers the projected area of the collector. Fig. 13 shows fog droplets trajectories as lines crossing the control volume. In this case, we are representing the trajectories of only 100 droplets per metre to facilitate visualisation; a larger number will produce merging of contiguous lines and the plot will look like a flat shade of grey.

The uneven separation of droplet trajectories after the mesh is caused by the particular starting points of each droplet coupled to the rather small number considered. However, this does not affect the results of collection efficiency. Indeed, de la Jara (2012) showed that the collection efficiency changes less than 1% when the number of droplets per metre considered in the simulation varies between 100 and 3000. Additionally, changes in the particular starting points of the droplets produce variations of less than 2% in the calculated efficiency.

The collection efficiencies obtained in the simulations are shown in Fig. 14. The efficiencies of the two MF-LFCs are higher than the one corresponding to the flat LFC because of the aerodynamic effects on two scales (de la Jara (2012)):

1. Collector scale: The shape of the module of the MF-LFC has a higher drag coefficient, increasing the aerodynamic efficiency of the collector, i.e. decreasing the fraction of droplets that go around the collector.
2. Fibre scale: The oblique orientation of the mesh with respect to wind direction increases the projected (i.e. perpendicular to the main direction of the flow) shade coefficient of the mesh from 30% for the flat LFC to 60% for the two MF-LFCs.

The collection efficiency of the closed MF-LFC is lower than the open version, in spite of its larger mesh area. This effect may be explained by the change in the droplets' trajectories near the fuse, where the incidence angle of the trajectories on the mesh decreases the projected area of

Table 1
Main constants used in the CFD simulation.

Variable	Value
Wind velocity	10 m/s
Droplet diameter	15 μm
LFC width	1 m
Mesh filament diameter	1 mm
Shade coefficient	30%
Air density	1.2 kg/m^3
Pressure	1 atm

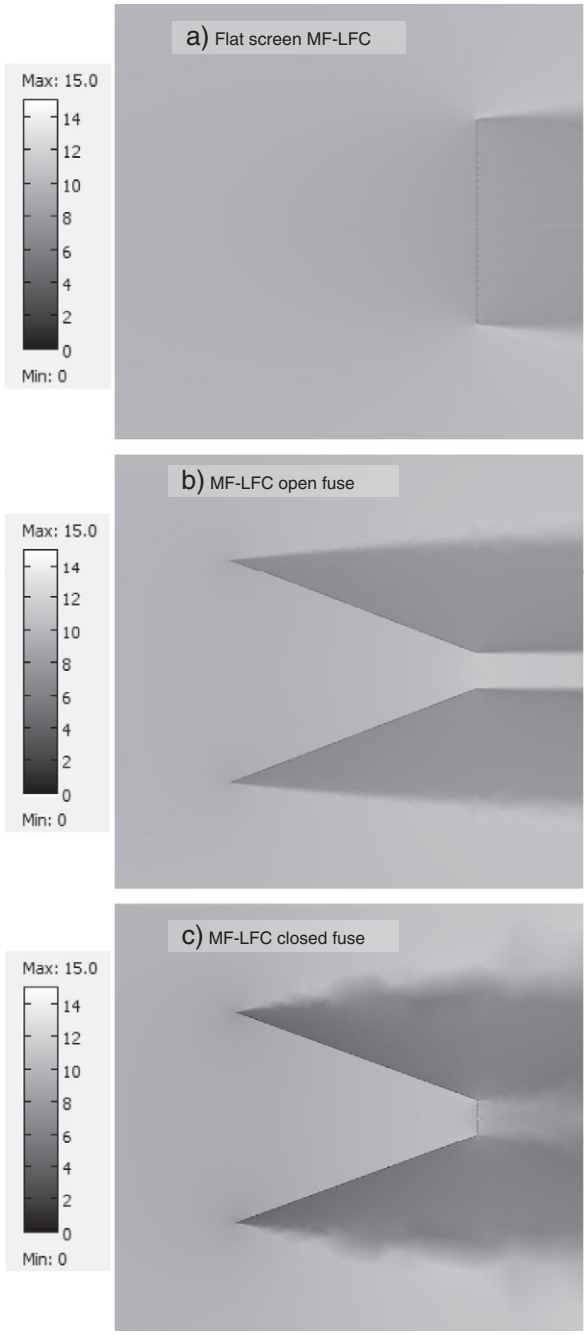

Fig. 11. Top-down view of velocity fields (m/s) over a 2-D geometry of fog collectors, wind unperturbed velocity = 10 m/s from left to right; the grey scale (left) shows the magnitude of the velocity. (a) Flat screen, normal wind. (b) Closed funnel, wind incidence angle on mesh 60°. (c) Open funnel, wind incidence angle on mesh 60°.

the fibres, thus, decreasing collection efficiency. On Fig. 15, the change of the trajectories is highlighted.

All simulations were performed considering single diameter droplets (15 μm), whilst fog has a characteristic size distribution (Schemenauer and Joe, 1989; Westbeld et al., 2009), in order to reduce computer memory and time requirements. The effect of this simplification on the collection efficiency is negligible and affects only the deposition efficiency, not the aerodynamic efficiency. Indeed, the deposition efficiency for 15 mm droplets impinging on a 1 mm circular filament is 90.88%, and for the droplet size distribution of Westbeld et al. (2009) is 91.50%, both calculated by the empirical correlation of Makkonen (1984). The aerodynamic collection efficiency

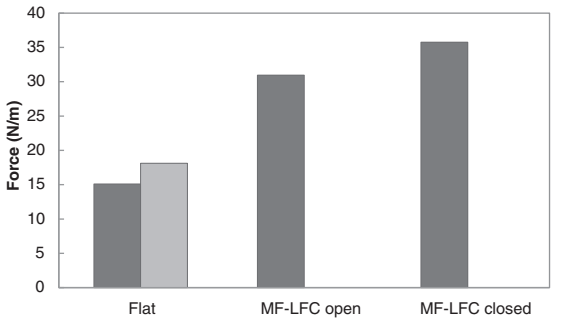

Fig 12. Total drag force per unit height of the structure for each type of LFC (N/m), obtained from CFD simulations. Light grey bar corresponds to Eq. (8).

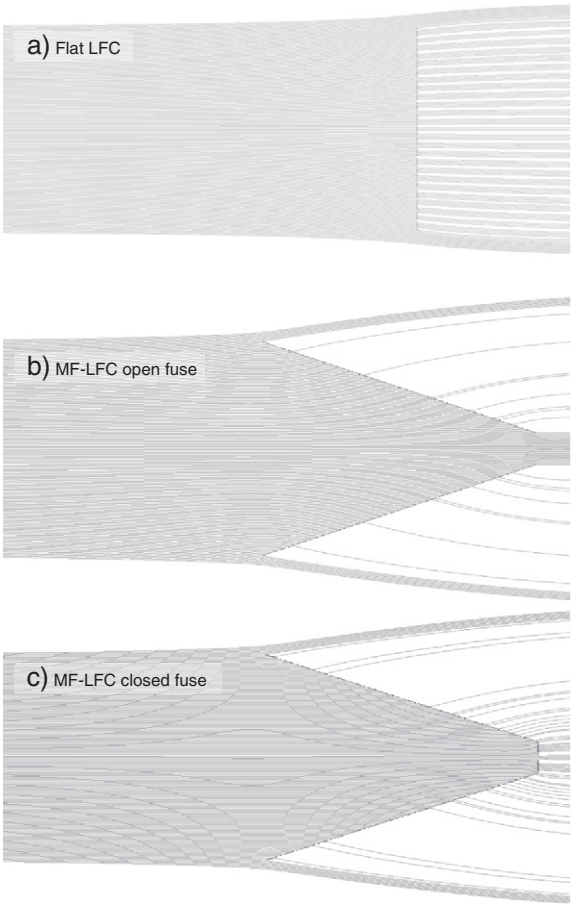

Fig. 13. Top-down view of fog droplets trajectories (grey lines) around and through the LFC (small black cylinders). (a) Flat, (b) MF open; (c) MF closed. In (b) and (c) only one of the funnel modules is shown.

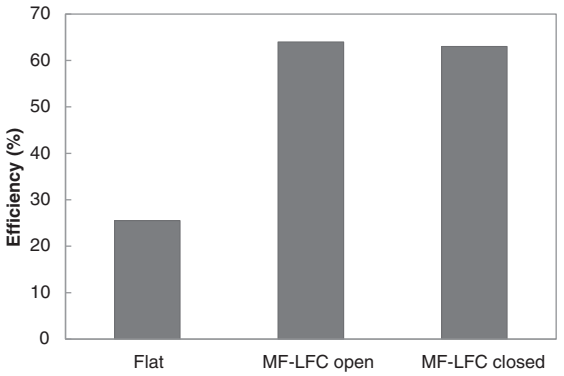

Fig. 14. Collection efficiency of three different collectors: Flat, 'Modular Funnel' open and closed. Every case considers collection area projected on a plane normal to wind velocity.

does not change since even the coarsest droplets will follow the wind streamlines around the collector, due to the scale of the LFC.

The proposed design is more complex than the conventionally flat LFC, but this complexity is compensated by larger collection efficiency and the ability to better resist strong winds, thanks to the tensegrity type structure. Indeed, tensegrity are structurally more efficient than conventional structures (Quirant et al., 2003; Ali et al., 2010).

To make a cost comparison between the proposed MF-LFC and the conventional, flat one, it is necessary to consider the total cost per unit water produced. This is equivalent to compare the cost per unit projected area divided by the collection efficiency. Fig. 14 shows that the efficiencies of the open MF-LFC and the flat one are 64% and 26%, respectively, which is a ratio of 2.5. Therefore, the cost per unit projected area of the former can be up to 2.5 times the cost of the latter to be a better choice cost-wise. In Table 2 we make a cost comparison between a flat LFC installed at Majada Blanca (Chile) in 2011, and the estimated cost of a MF-LFC of the same projected area (150 m^2). The MF-LFC has total mesh area 1.76 times the conventional one, and the total cost increases by a factor of 1.24, but the rate of water collected increases in by a factor of 2.46. This means that the cost of the litre of water collected by the MF-LFC should be one half of the cost corresponding to the flat LFC. In summary, the MF-LFC should have a clear advantage over the conventional one.

6. Conclusions

1. The new MF-LFC morphology considers smaller mesh surface elements in comparison to the large continuous surface in the flat screen of the traditional LFC. This implies a decrease in the stress on the mesh fibres due to wind pressure, which improves the functional performance of the system.
2. With the funnel morphology of the MF-LFC there is an improvement of the wind driven fog flux in relation to the traditional LFC version where the average wind speed at the mesh surface is lower due to the blockage effect. This improves water collection due to the increase of the drag coefficient and by providing flux continuity.
3. The MF-LFC with an open funnel vertex has a lower drag force than with a closed funnel vertex (31 N/m and 36 N/m, respectively), and a slightly higher collection efficiency than with a closed vertex (64% and 63%, respectively), therefore open is better than closed.
4. The MF-LFC with an open funnel vertex has higher drag force than the flat LFC (30.95 N/m and 15.1 N/m, respectively). Also it has a much higher collection efficiency (64% and 26%, respectively), therefore it seems to be the most convenient of the three designs analysed in this study.
5. Both open and closed funnel vertex MF-LFCs have larger drag force than a flat LFC, therefore from the structural point of view there is no improvement. However, this is compensated by the decrease of the stresses due to the smaller mesh surfaces.
6. The design of the tensile structure optimises the efficiency of material use in the MF-LFC in relation to the resistance to strong winds. This optimisation also has a direct impact on the material resources, production, erection and maintenance processes which are finally reflected in the cost of water as the end product.
7. The comparison of the cost per unit water produced of the MF-LFC and the conventional LFC, which is related to their efficiencies, seems to favour the first one.

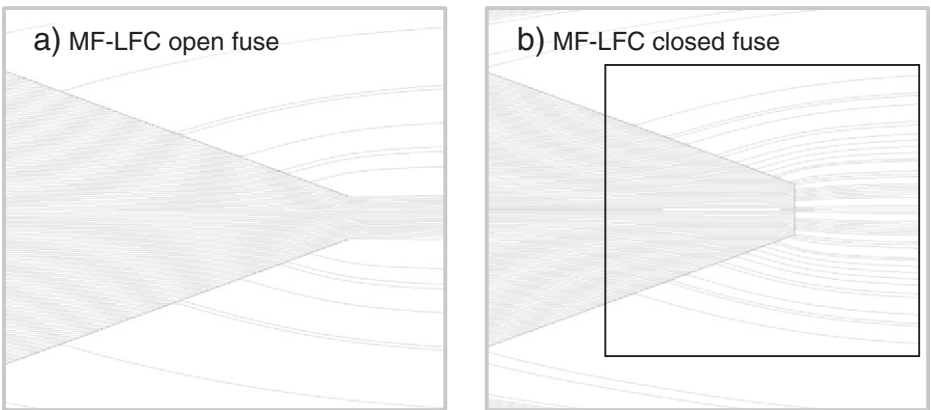

Fig. 15. The disturbance of droplets trajectories by the closed fuse on the MF-LFC highlighted by the black rectangle on panel b.

Table 2
Cost comparison between a typical flat LFC and a modular funnel LFC, both with 150 m^2 of frontal area (projected area).

	Flat		Modular funnel	
Item	USD	%	USD	%
Structure	2 002	28.8	2 326	27.0
Cables	652	9.4	1 375	15.9
Trough	60	0.9	107	1.2
Mesh	206	3.0	363	4.2
Erection (labour, transp., materials)	4 035	58.0	4 457	51.7
Total	6 956	100.0	8 628	100.0
Total cost per m^2 frontal area	46.4		57.5	

Acknowledgements

The authors want to acknowledge the support of Vicerrectoria de Investigación of Pontificia Universidad Católica de Chile that funded the project "Estrategias de diseño para la optimización de Colectores de Agua de Niebla," and Professor Diego López-García that contributed with structural aspects. They also want to acknowledge the valuable contribution of the reviewers, which with their comments and observations helped to significantly improve the quality of this paper.

References

Abdul-Wahab, S.A., Lea, V., 2008. Reviewing fog water collection worldwide and in Oman. Int. J. Environ. Stud. 65, 485–498.
Abdul-Wahab, S.A., Al-Damkhi, A.M., Al-Hinai, H., Al-Najar, K.A., Al-Kalbani, M.S., 2010. Total fog and rainwater collection in the Dhofar region of the Sultanate of Oman during the monsoon season. Water Int. 35, 100–109.
Agustsson, H., Olafsson, H., 2009. Forecasting wind gusts in complex terrain. Meteorol. Atmos. Phys. 103, 173–185. http://dx.doi.org/10.1007/s00703-008-0347-y.
Al-hassan, G.A., 2009. Fog water collection evaluation in Asir Region–Saudi Arabia. Water Resour. Manage. 23, 2805–2813. http://dx.doi.org/10.1007/s11269-009-9410-9.
Ali, N.B.H., Rhode-Barbarigos, L., Albi, A.A.P., Smith, I.F.C., 2010. Design optimization and dynamic analysis of a tensegrity-based footbridge. Eng. Struct. 32, 3650–3659.
Boettcher, F., Renner, Ch., Waldl, H.P., Peinke, J., 2003. On the statistics of wind gusts. Bound.-Lay. Meteorol. 108, 163–173.
Bresci, E., 2002. Wake characterization downstream of a fog collector. Atmos. Res. 64, 217–225.
Briassoulis, D., Mistriotis, A., Giannoulis, A., 2010. Wind forces on porous elevated panels. J. Wind Eng. Ind. Aerodyn. 98, 919–928.
Cereceda, P., Osses, P., Larrain, H., Farías, M., Lagos, M., Pinto, R., Schemenauer, R.S., 2002. Advective, orographic and radiation fog in the Tarapacá region, Chile. Atmos. Res. 64, 261–271.
Cereceda, P., Larrain, H., Osses, P., Farías, M., Egaña, I., 2008a. The climate of the coast and fog zone in the Tarapacá Region, Atacama Desert, Chile. Atmos. Res. 87, 301–311.
Cereceda, P., Larrain, H., Osses, P., Farías, M., Egaña, I., 2008b. The spatial and temporal variability of fog and its relation to fog oasis in the Atacama Desert, Chile. Atmos. Res. 87, 312–323.
Comsol, A.B., 2008. ComsolMultiphysics, version 3.5a (3.5.0.603–2008/12/03). Available from http://www.comsol.com/.
de la Jara, E., 2012. Modelación computacional del impacto de gotas de niebla en fibras cilíndricas paralelas. (M. Sc. Thesis) Pontificia Universidad Católica de Chile, Santiago, Chile.
de la Lastra, C., 2002. Report on the fog-collecting project in Chungungo: assessment of the feasibility of assuring its sustainability. International Development Research Centre (IDRC), Ottawa, Ont, Canada (online).
Estrela, M.J., Valiente, J.A., Corell, D., Millán, M.M., 2008. Fog collection in the western Mediterranean basin (Valencia region, Spain). Atmos. Res. 87, 324–337.
Gandhidasan, P., Abualhamayel, H.I., 2006. Fog collection as a source of fresh water supply in the Kingdom of Saudi Arabia. Water Environ. J. 21 (2007), 19–25. http://dx.doi.org/10.1111/j.1747-6593.2006.00041.x.
Giannouilis, A., Stathopoulos, T., Briassoulis, D., Mistriotis, A., 2012. Wind loading on vertical panels with different permeabilities. J. Wind Eng. Ind. Aerodyn. 107–108, 1–16.
Gischler, C., 1991. The missing link in a production chain, vertical obstacles to catch Camanchaca. ROSTLAC-UNESCO, Montevideo – Uruguay ISBN 92-9089-019-7.
Heisler, G.M., Dewalle, D.R., 1988. Effects of windbreak structure on wind flow. Agric. Ecosyst. Environ. 22/23, 41–69.
Klemm, O., Schemenauer, R.S., Lummerich, A., Cereceda, P., Marzol, V., Corell, D., van Heerden, J., Reinhard, D., Gherezghiher, Tseggai, Olivier, Jana, Osses, Pablo, Sarsour, Jamal, Frost, Ernst, Estrela, M.J., Valiente, J.A., Fessehaye, G.M., 2012. Fog as a fresh-water resource: overview and perspectives. Ambio. http://dx.doi.org/10.1007/s13280-012-0247-8 (Royal Swedish Academy of Sciences).
Larrain, H., Velásquez, P., Cereceda, P., Espejo, R., Pinto, R., Osses, P., Schemenauer, R.S., 2002. Fog measurements at the site "Falda Verde" north of Chañaral compared with other fog stations of Chile. Atmos. Res. 64, 273–284.
LeBoeuf, R., Rivera, J.D., de-la-Jara, E., 2013. 6th International Conference on Fog, Fog Collection, and Dew, Yokohama, Japan.
Letchford, C., 2001. Wind loads on rectangular signboards and hoardings. J. Wind Eng. Ind. Aerodyn. 89 (2), 135–151 (Available at: http://linkinghub.elsevier.com/retrieve/pii/S0167610500000684).
Letchford, C.W., et al., 2000. Mean wind loads on porous canopy roofs. J. Wind Eng. Ind. Aerodyn. 84 (2), 197–213 (Available at: http://linkinghub.elsevier.com/retrieve/pii/S0167610599001038).
Louw, C., van Heerden, J., Olivier, J., 1998. The South African fog-water collection experiment: Meteorological features associated with water collection along the eastern escarpment of South Africa. Water SA 24, 269–280.
Makkonen, L., 1984. Modelling of ice accretion on wires. J. Clim. Appl. Meteorol. 23, 929–939.
Marzol, M.V., 2002. Fog water collection in a rural park in the Canary Islands (Spain). Atmos. Res. 64, 239–250.
Marzol, M.V., 2008. Temporal characteristics and fog water collection during summer in Tenerife (Canary Islands, Spain). Atmos. Res. 87, 352–361.
Marzol, M.V., Sánchez, J.L., 2008. Fog water harvesting in Ifni, Morocco. An assessment of potential and demand. Die Erde 139, 97–119.
Michna, P., Schenk, J., Werner, R.A., Eugster, W., 2013. MiniCASCC — A battery driven fog collector for ecosystem research. Atmos. Res. 128, 24–34.
Olivier, J., 2002. Fog-water harvesting along the West Coast of South Africa: A feasibility study. Water SA 28, 349–360.
Olivier, J., de Rautenbach, C.J., 2002. The implementation of fog water collection systems in South Africa. Atmos. Res. 64, 227–238.
Park, K.-C., Chhatre, S.S., Srinivasan, S., Cohen, R.E., McKinley, G.H., 2013. Optimal design of permeable fiber network structures for fog harvesting. Langmuir 29, 13269–13277. http://dx.doi.org/10.1021/la402409f.
Petersen, E.L., Mortensen, N.G., Landberg, L., Hojstrup, J., Frank, H.P., 1998. Wind power meteorology. Part I: Climate and turbulence. Wind Energy 1 (1), 25–45 (Available at: http://doi.wiley.com/10.1002/(SICI)1099-1824(199809)1:1<2::AID-WE15>3.0.CO;2-Y).
Quirant, J., Kazi-Aoual, M.N., Motro, R., 2003. Designing tensegrity systems: The case of a double layer grid. Eng. Struct. 25, 1121–1130.
Richards, P., Robinson, M., 1999. Wind loads on porous structures. J. Wind Eng. Ind. Aerodyn. 83 (1-3), 455–465 (Available at: http://linkinghub.elsevier.com/retrieve/pii/S0167610599000938).
Rivera, J.D., 2011. Aerodynamic collection efficiency of fog water collectors. Atmos. Res. 102, 335–342. http://dx.doi.org/10.1016/j.atmosres.2011.08.005.
Schemenauer, R.S., Cereceda, P., 1994a. The role of wind in rainwater catchment and fog collection. Water Int. 19, 70–76.
Schemenauer, R.S., Cereceda, P., 1994b. A proposed standard fog collector for use in high-elevation regions. J. Appl. Meteorol. 33, 1313–1322.
Schemenauer, R.S., Joe, P.I., 1989. The collection efficiency of a massive fog collector. Atmos. Res. 24, 53–69.
Schemenauer, R.S., Fuenzalida, H., Cereceda, P., 1988. A neglected water resource: The Camanchaca of South America. Bull. Am. Meteorol. Soc. 69, 138–147.
Schemenauer, R.S., Cereceda, P., Osses, P., 2005. Fog Water Collection Manual. FogQuest, Ontario, Canada (www.fogquest.org (2005)).
Shanyengana, E.S., Henschel, J.R., Seely, M.K., Sanderson, R.D., 2002. Exploring fog as a supplementary water source in Namibia. Atmos. Res. 64, 251–259.
Uematsu, Y., Stathopoulos, T., Iizumi, E., 2008. Wind loads on free-standing canopy roofs: Part 1 local wind pressures. J. Wind Eng. Ind. Aerodyn. 96 (6-7), 1015–1028 (Available at: http://linkinghub.elsevier.com/retrieve/pii/S016761050700150X [Accessed April 29, 2013]).

United Nations, 2008. The millenium development goals report. Retrived from: http://www.un.org/millenniumgoals/pdf/The%20Millennium%20Development%20Goals%20Report%202008.pdf.
Walshaw, D., Anderson, C.W., 2000. A model for extreme wind gusts. Appl. Stat. 49 (Part 4), 499–508.
Weggel, J.R., 1999. Maximum daili wind gusts related to mean daily wind speed. J. Struct. Eng. 125, 465–468.
Westbeld, A., Klemm, O., Grießbaum, F., Sträter, E., Larrain, H., Osses, P., Cereceda, P., 2009. Fog deposition to a *Tillandsia* carpet in the Atacama Desert. Ann. Geophys. 27, 3571–3576.
White, F.M., 1986. Fluid Mechanics, second ed. McGraw-Hill Book Company, New York.